Journal of Cerebral Blood Flow & Metabolism (2010) 30, 969–984

www.jcbfm.com

Role of Nogo-A in neuronal survival in the reperfused ischemic brain

Ertugrul Kilic[1,2,3,5], Ayman ElAli[1,2,5], Ülkan Kilic[2,3], Zeyun Guo[2], Milas Ugur[3], Unal Uslu[3], Claudio L Bassetti[2], Martin E Schwab[4] and Dirk M Hermann[1,2]

[1]*Department of Neurology, University Hospital Essen, Essen, Germany;* [2]*Departement of Neurology, University Hospital Zurich, Zurich, Switzerland;* [3]*Departments of Physiology, Histology and Embryology, Yeditepe University, Istanbul, Turkey;* [4]*Brain Research Institute, University of Zurich, Zurich, Switzerland*

Nogo-A is an oligodendroglial neurite outgrowth inhibitor, the deactivation of which enhances brain plasticity and functional recovery in animal models of stroke. Nogo-A's role in the reperfused brain tissue was still unknown. By using Nogo-A$^{-/-}$ mice and mice in which Nogo-A was blocked with a neutralizing antibody (11C7) that was infused into the lateral ventricle or striatum, we show that Nogo-A inhibition goes along with decreased neuronal survival and more protracted neurologic recovery, when deactivation is constitutive or induced 24 h before, but not after focal cerebral ischemia. We show that in the presence of Nogo-A, RhoA is activated and Rac1 and RhoB are deactivated, maintaining stress kinases p38/MAPK, SAPK/JNK1/2 and phosphatase-and-tensin homolog (PTEN) activities low. Nogo-A blockade leads to RhoA deactivation, thus overactivating Rac1 and RhoB, the former of which activates p38/MAPK and SAPK/JNK1/2 via direct interaction. RhoA and its effector Rho-associated coiled-coil protein kinase2 deactivation in turn stimulates PTEN, thus inhibiting Akt and ERK1/2, and initiating p53-dependent cell death. Our data suggest a novel role of Nogo-A in promoting neuronal survival by controlling Rac1/RhoA balance. Clinical trials should be aware of injurious effects of axonal growth-promoting therapies. Thus, Nogo-A antibodies should not be used in the very acute stroke phase.
Journal of Cerebral Blood Flow & Metabolism (2010) **30,** 969–984; doi:10.1038/jcbfm.2009.268; published online 20 January 2010

Keywords: neuroprotection; neuronal signaling; signal transduction; stress proteins; cerebral ischemia and/or reperfusion

Introduction

Oligodendroglial inhibitors of neurite outgrowth have obtained considerable interest in the treatment of spinal cord trauma and ischemic stroke recently (Schwab, 2004; Buchli and Schwab, 2005; Yiu and He, 2006; Harel and Strittmatter, 2006). Several proteins with repulsive or inhibitory effects on growing neurites have been identified in the adult central nervous system (Yiu and He, 2006). Among these, the myelin membrane protein Nogo-A has been shown to prevent axonal regeneration and plasticity in a particularly powerful way *in vivo* (Schwab, 2004; Buchli and Schwab, 2005; Yiu and He, 2006; Harel and Strittmatter, 2006).

The *nogo* gene generates three main proteins, Nogo-A, -B, and -C, but only Nogo-A has potent neurite growth inhibitory activity and a distribution that is mostly central nervous system central nervous system specific (Chen *et al*, 2000; GrandPré *et al*, 2000). The functions of Nogo-B and -C are largely unknown. It has been suggested that Nogo-B controls angiogenesis, promoting the migration of endothelial cells but inhibiting that of vascular smooth muscle cells (Acevedo *et al*, 2004).

Inhibition of Nogo-A with neutralizing antibodies potently enhanced axonal sprouting and neurologic recovery in rodent and primate models of spinal cord trauma (Schnell and Schwab, 1990; Bregman *et al*, 1995; Merkler *et al*, 2001; Liebscher *et al*, 2005; Freund *et al*, 2006) and ischemic stroke (Papadopoulos *et al*, 2002; Wiessner *et al*, 2003; Markus *et al*, 2005; Seymour *et al*, 2005). Hopes have emerged from these data that Nogo-A inhibition may facilitate neurologic recovery also in human patients. A clinical trial with Nogo-A antibodies in spinal cord trauma is currently in progress.

In view that all hitherto performed studies in stroke were performed in permanent stroke models, we recently aimed to characterize the plasticity-promoting effects of Nogo-A$^{-/-}$ after transient focal

Correspondence: Professor DM Hermann, Department of Neurology, University Hospital Essen, Hufelandstr. 55, D-45122 Essen, Germany.
E-mail: dirk.hermann@uk-essen.de
[5]These authors contributed equally to this work.
Received 16 April 2009; revised 27 November 2009; accepted 2 December 2009; published online 20 January 2010

cerebral ischemia. Strikingly, Nogo-A$^{-/-}$ mice submitted to 30 mins middle cerebral artery (MCA) occlusion revealed an increased mortality, associated with exacerbated neurologic deficits, when compared with wild-type (WT) animals. On the basis of these findings, we evaluated the effect of NogoA$^{-/-}$ as well as of an acute antibody-mediated Nogo-A deactivation on neuronal injury and neurologic recovery in the reperfused ischemic brain.

Rho GTPases have an important function in neuronal plasticity (McGee and Strittmatter, 2003). As such, activation of the Nogo-66 receptor stimulates the small GTPase RhoA, thus inhibiting axonal growth (McGee and Strittmatter, 2003). The link between Nogo and Rho GTPases prompted us to test, whether and how small GTPases are involved in Nogo-A's neuronal survival-promoting activities. As such, we evaluated the expression and activation of the GTPases RhoA, RhoB, and Rac1 and tested how these signal factors interact with known cell death pathways. As a result of these experiments, we here report a hitherto unknown role of Nogo-A in controlling neuronal survival after transient focal cerebral ischemia.

Materials and methods

Animal Groups

All experiments were performed with governmental approval (Kantonales Veterinäramt Zürich, ZH169/2005) according to the NIH guidelines for care and use of laboratory animals. In a first set of studies, we submitted male Nogo-A$^{-/-}$ mice with a pure C57Bl/6 strain background (Dimou *et al*, 2006, Simonen *et al*, 2003), and their WT littermates (all 23 to 28 g) to 30 mins MCA occlusion followed by 96 h reperfusion ($n=8$ animals/group). In view that Nogo-A$^{-/-}$ animals exhibited increased dropout rates (see Results section) and exacerbated neuronal injury, considering that Nogo-A$^{-/-}$ mice might show compensatory changes that may be responsible for the increased neuronal injury, we subsequently treated male C57Bl/6 mice (21 to 24 g) with purified mouse monoclonal Nogo-A antibody (11C7; kindly provided by Novartis, Basle, Switzerland) (Oertle *et al*, 2003; Liebscher *et al*, 2005) or control IgG, by infusing the antibodies (1) into the lateral ventricle ipsilateral to the stroke or (2) into the ischemic striatum, treatment starting immediately after reperfusion (post-ischemic groups), or (3) into the ipsilateral lateral ventricle, antibody delivery being initiated 24 h before MCA occlusion (pre-ischemic groups) ($n=8$ animals/group). These animals were killed at 72 h after the MCA occlusion.

The slightly longer reperfusion time in case of Nogo-A$^{-/-}$ studies as compared with the antibody-treated animals resulted from the fact that the decision to kill the animals was made on day 3 after stroke, when animal dropouts were noted. As such, animals were killed the next day. The delivery of the Nogo-A antibody into the lateral ventricle closely reflects the intrathecal route of application that is used clinically in patients with spinal cord trauma (Buchli and Schwab, 2005). The intrastriatal delivery was chosen to maximally expose brain neurons with Nogo-A antibody. We thereby wanted to test whether survival effects of the antibody may be stronger when the antibody is present in the tissue at high concentration.

As part of more thorough behavioral assessments, in an effort to characterize neuronal survival by computer-based stereological analysis, additional mice received infusions of 11C7 antibody or control IgG into the lateral ventricle ipsilateral to the stroke starting 24 h before MCA occlusion ($n=8$ animals/group). These animals were killed 7 days after reperfusion.

Induction of Intraluminal Middle Cerebral Artery Occlusion

For induction of focal cerebral ischemia, animals were anesthetized with 1% halothane (30% O_2, remainder N_2O). Rectal temperature was maintained between 36.5 and 37.0°C using a feedback-controlled heating system. During the experiments, laser Doppler flow (LDF) was monitored using a flexible 0.5 mm fiberoptic probe (Perimed, Stockholm, Sweden) attached to the intact skull overlying the MCA territory (2 mm posterior/6 mm lateral from bregma). The LDF changes were measured during 30 mins of MCA occlusion and up to 15 mins after reperfusion onset. Focal cerebral ischemia was induced using an intraluminal filament technique, as described (Kilic *et al*, 2005, 2006; Spudich *et al*, 2006). Briefly, a midline neck incision was made, and the left common and external carotid arteries were isolated and ligated. A microvascular clip (FE691, Aesculap, Tuttlingen, Germany) was temporarily placed on the internal carotid artery. A 8-0 nylon monofilament (Ethilon; Ethicon, Norderstedt, Germany) coated with silicon resin (Xantopren, Bayer Dental, Osaka, Japan; diameter of the coated suture: 180 to 200 μm) was introduced through a small incision into the common carotid artery and advanced 9 mm distal to the carotid bifurcation for MCA occlusion. Thirty minutes after MCA occlusion, reperfusion was initiated by withdrawal of the monofilament.

Delivery of Monoclonal Mouse Nogo-A Antibody

Immediately after the stroke (i.e., after terminating the LDF recordings) or at 24 h before ischemia, cannulae linked to miniosmotic pumps (Alzet 1003D or 1007D, Palo Alto, CA, USA) were implanted under halothane anesthesia into the left-sided lateral ventricle (1 mm lateral to bregma/2.5 mm below brain surface) or the left-sided striatum (2.4 mm lateral to bregma level/2.5 mm below brain surface) of C57Bl/6 mice, via which purified monoclonal mouse Nogo-A antibody (11C7) or control mouse IgG was subsequently applied. In all animals, a bolus of 6 μg control IgG or Nogo-A antibody was administered during the pump implantation, followed by continuous infusion of 3 μg/h antibody over the subsequent days. As such, antibodies were dissolved at a concentration of 3 μg/μL (Alzet 1003D; used for MCA occlusion/3 days reperfusion studies) or 6 μg/μL (Alzet 1007D; MCA occlusion/7 days reperfusion

studies), taking into account that the infusion rate was 1 μL/h (Alzet 1003D) and 0.5 μL/h (Alzet 1007D). After the implantation, wounds were carefully sutured. Anesthesia was discontinued and animals were placed back into their cages.

Behavioral Tests

Grip Strength Test: The grip strength test consists of a spring balance coupled with a Newtonmeter (Medio-Line Spring Scale, metric, 300 g, Pesola AG, Switzerland) that is attached to a triangular steel wire, which the animal instinctively grasps. When pulled by the tail, the animal exerts force on the steel wire (Tremml *et al*, 1998). Grip strength was evaluated at the right paretic forepaw of mice submitted to left-sided MCA occlusion, the left non-paretic forepaw being wrapped with adhesive tape. Grip strength was evaluated five times on occasion of each test, which took place on the day before stroke (all animals), on day 3 (all animals) and day 7 (animals kept for detailed behavioral analysis) after MCA occlusion. For all five measurements, mean values were calculated. From these data, percentage values (post-ischemic versus pre-ischemic baseline) were computed. Pre-ischemic results did not reveal any differences between groups.

RotaRod Test: As part of a more detailed behavioral analysis, we investigated motor coordination on a RotaRod in animals pretreated with Nogo-A antibody 24 h before MCA occlusion. The RotaRod consists of a rotating drum with a speed accelerating from 4 to 40 rpm (Ugo Basile, model 47600, Comerio, Italy; Sugiura *et al*, 2005). Maximum speed is reached after 245 secs, and the time at which the animal drops off the drum is evaluated (maximum testing time: 300 secs). Measurements were performed on the same occasion as grip strength tests, i.e., before pump implantation, at 3 and 7 days after MCA occlusion. For all five measurements, mean values were again computed, from which percentage values (post-ischemic versus pre-ischemic) were calculated. Pre-ischemic data did not differ between groups.

Open Field Test: In animals subjected to a more detailed behavioral analysis, spontaneous locomotor activity was also evaluated by means of an open field test (Kilic *et al*, 2008). The open field consists of a square arena (diameter: 120 cm) surrounded by a wall. The arena is divided into two sections, including an outer wall zone and an inner center zone. Each mouse was released near the wall and observed for 10 mins. Animal paths were tracked with an electronic imaging system (Ethovision XT6; Noldus Information Technology, Wageningen, Netherlands). To characterize animal activity, the total time progressing and the distance moved were evaluated (Bergh *et al*, 2007; Kilic *et al*, 2008). Animals were tested before pump implantation, as well as on days 3 and 7 after MCA occlusion.

Elevated Plus Maze: In the latter animals, exploration behavior was finally assessed on an elevated plus maze. This test detects correlates of fear and anxiety, besides locomotor behavior (Young *et al*, 2008). The plus maze is made of plexiglas, which consists of four arms (two open arms without walls and two arms enclosed by 15 cm high walls), which are 30 cm long and 5 cm wide. Each arm of the maze is attached to plexiglas legs such that it is elevated 40 cm above the table. Animals were placed in one of the protected sectors and observed for 10 mins. Times spent in unprotected sector were analyzed whenever the animal moved into it with all four paws. Exploration behavior was assessed on the elevated plus maze after the stroke on the same days when RotaRod and open field tests were performed.

Animal Sacrifice

For conventional histochemical and molecular biological studies, animals were re-anaesthetized with halothane and decapitated at 96 h (WT or Nogo-A$^{-/-}$ mice) or 72 h (mice receiving control IgG or Nogo-A antibody by infusion into lateral ventricle or striatum) after the stroke. Brains were removed, frozen on dry ice, and cut on a cryostat into coronal 18 μm sections that were used for studying brain distribution of the Nogo-A antibody, for terminal transferase biotinylated-dUTP nick end labeling (TUNEL) and immunohistochemistry of the neuronal nuclear protein NeuN. From the same animals, tissue samples were taken from the MCA territory (striatum and overlying parietal cortex) both ipsilateral and contralateral to the stroke for protein expression and interaction studies.

For computer-based stereological analysis of NeuN+ cells in the striatum, animals receiving infusions of control or neutralizing NogoA antibody into the lateral ventricle starting 24 h before MCA occlusion were killed by transcardiac perfusion with 0.1 mol/L phosphate-buffered saline (PBS) followed by a fixative containing 4% paraformaldehyde in 0.1 mol/L PBS at 7 days after the stroke. Brains were removed, post-fixed overnight in 2% paraformadehyde in 0.1 mol/L PBS and cryoprotected by immersion in 20% sucrose solution. Brains were frozen and cut on a cryostat into coronal 40 μm sections.

Nogo-A Antibody Distribution Studies

With gentle stirring, brain sections from the level of the mid-striatum (bregma 0.0 mm) of animals killed by decapitation at 96 or 72 h after MCA occlusion were rinsed for 10 mins at room temperature in 0.1 mol/L PBS to remove intravascular IgG, and fixed for 20 mins at 4°C with 4% paraformaldehyde/0.1 mol/L PBS (Kilic *et al*, 2006). Following blockade of endogenous peroxidase with methanol/0.3% H_2O_2 and immersion in 0.1 mol/L PBS containing 5% bovine serum albumin and normal swine serum (1:1000), sections were incubated for 1 h in biotinylated anti-mouse IgG (Santa Cruz Biotechnology, Nunningen, Switzerland) and stained with an avidin peroxidase kit (Vectastain Elite; Vector Laboratories, Burlingname, CA, USA) and diaminobenzidine (DAB; Sigma, Deisenhofen, Germany). After coverslipping, sections were scanned and evaluated by

analyzing the maximum dorsoventral and lateral extension of the Nogo-A antibody covered tissue area.

Analysis of DNA Fragmented Cells

Brain sections obtained from the mid-striatum of animals killed at 96 or 72 h after MCA occlusion were fixed for 20 mins at 4°C with 4% paraformaldehyde/0.1 mol/L PBS. The TUNEL staining was then performed, as described earlier (Hermann *et al*, 2001; Wang *et al*, 2005). Briefly, after labeling with terminal desoxynucleotidyl transferase mix, containing 12.5 mg/mL terminal desoxynucleotidyl transferase (Boehringer-Mannheim, Mannheim, Germany) and 25 mg/mL biotinylated dUTP (Boehringer-Mannheim), sections were stained with streptavidin-FITC, counterstained with 4′,6-diamidino-2-phenylindole (DAPI) and coverslipped. Injured cells were microscopically evaluated by counting the density of DNA-fragmented profiles in predefined arrays consisting of (1) 12 regions of interest (ROI) in the ischemic striatum, 250 μm apart, (2) three ROI in the basal forebrain, 250 μm apart, and (3) in five random ROI in the cerebral cortex, 250 μm apart (each ROI measuring 62,500 μm^2) (Figure 1M). Data analysis was performed by two investigators blinded for the experimental condition (ÜK, EK; blinding ensured by taping the animal numbers on the object slides). Mean values were calculated for all areas and both cells counting.

Immunohistochemistry for NeuN

Adjacent brain sections of the same animals were fixed in 4% paraformaldehyde/0.1 mol/L PBS, washed and immersed for 1 h in 0.1 mol/L PBS containing 0.3% Triton X-100 (PBS-T)/10% normal goat serum. Sections were incubated overnight at 4°C with monoclonal mouse anti-NeuN (MAB377; Chemicon, Lucerne, Switzerland; 1:100 in PBS-T, used for Nogo-$A^{-/-}$ studies) antibody, which was detected with anti-mouse Cy3 antibody, or with Alexa Fluor@488 monoclonal mouse anti-NeuN antibody (MAB377XMSX; Chemicon; 1:100 in PBS-T, used for Nogo-A antibody studies due to 11C7 antibody crossreactions). Sections were finally incubated with DAPI and coverslipped. Surviving neurons were microscopically evaluated by two blinded researchers (ÜK, EK) by counting the density of NeuN neurons in the same random ROI as above (Figure 1M), both ipsilateral and contralateral to the stroke. Mean values were calculated for all areas. With these data, the percentage of surviving neurons was determined for each structure.

For computer-based stereological analysis, six equidistant sections of the striatum, 480 μm apart, obtained from mice killed by transcardiac perfusion with 4% paraformaldehyde 7 days after the stroke were boiled in 0.01 mol/L citrate buffer for 15 mins for epitope retrieval. Sections were incubated in 0.3% H_2O_2 for 10 mins, followed by 5% normal goat serum for 30 mins. Sections were incubated for 60 mins in anti-NeuN antibody (MAB 377, Chemicon), diluted 1:100 in 5% normal goat serum in 0.3% Triton X-100/0.1 mol/L PBS for 60 min. Sections were immersed with Vectastain AB kit (Vector Laboratories) and stainings developed with diaminobenzidine tetrahydrochloride (DAKO, Carpinteria, CA, USA).

Computer-based Stereology of NeuN+ Cells in Ischemic Striatum

The focal plane of the objective lens was focused down through the sections from top to bottom. When the first neuronal nucleus came into focus at the top, the microcator was zeroed and focused further down until the processes slipped out of focus at the bottom where the distance was read on the microcator. As such, the thickness of brain sections was determined at various positions of the striatum. The mean thickness was 36 μm, pointing toward some minor shrinkage of the brain sections to 90%. The mean thickness t of individual animals and the height of the optical dissector h were the basis of calculating the thickness sampling fraction *tsf*, which is the ratio h/t.

Cell numbers were quantified according to the optical fractionator method using Stereo Investigator 7.5 software (MicroBrightField, Inc, Colchester, VT, USA) on a personal computer connected to a color video camera mounted on a Leica DM 4000 microscope (Bacigaluppi *et al*, 2009). The motorized stage of the microscope, which was controlled by the software, allowed precise and well-defined movements along the *x*-, *y*- and *z*-axes. Images were first acquired with a CCD-IRIS color video camera and the striatum was interactively delineated at low magnification on a video image of the section. The counting was performed using a $\times 63$ oil immersion lens.

The computer-controlled microscope stage was programmed to position optical dissector probes in a systematic random pattern within the delineated field of the histologic section. The sampling interval, i.e., the X and Y distances between the dissector probes, was kept constant within each structure of the same brain and chosen so that $\sim$400 neurons were counted on average. Guard volumes of 2 μm at the top of the section were used to avoid problems related to surface artifacts.

Only cells that came into focus within the volume of the dissector, as one focused through the height of the optical dissector (15 μm), were counted. The total number of cells (N) was estimated both ipsilateral and contralateral to the stroke using the equation: $N = \Sigma Q^- \times 1/tsf \times 1/asf \times 1/ssf$, where ΣQ^- is the total number of neurons counted, *tsf* is the thickness sampling fraction, *asf* is the area sampling faction, and *ssf* is the section sampling fraction. Thereby, the percentage of surviving neurons in the ischemic striatum was calculated.

In addition to the stereological analysis of neuronal densities, a volumetric analysis of the striatum was performed by outlining the outer border of the striatum on all six sections, thus analyzing the expansion of the striatum throughout its rostrocaudal extension. From the areas measured, striatal volumes were calculated.

Protein Expression and Interaction Studies

Antibodies and Chemicals: For protein expression and interaction studies, the following antibodies and chemicals were used: anti-Nogo-A (sc-25660), anti-RhoB (sc-180), and anti-Rho-associated coiled-coil protein kinase-2 (Rock2) (sc-1851) antibodies, as well as A/G plus-agarose (sc-2003) were purchased from Santa Cruz Biotechnology. Recombinant

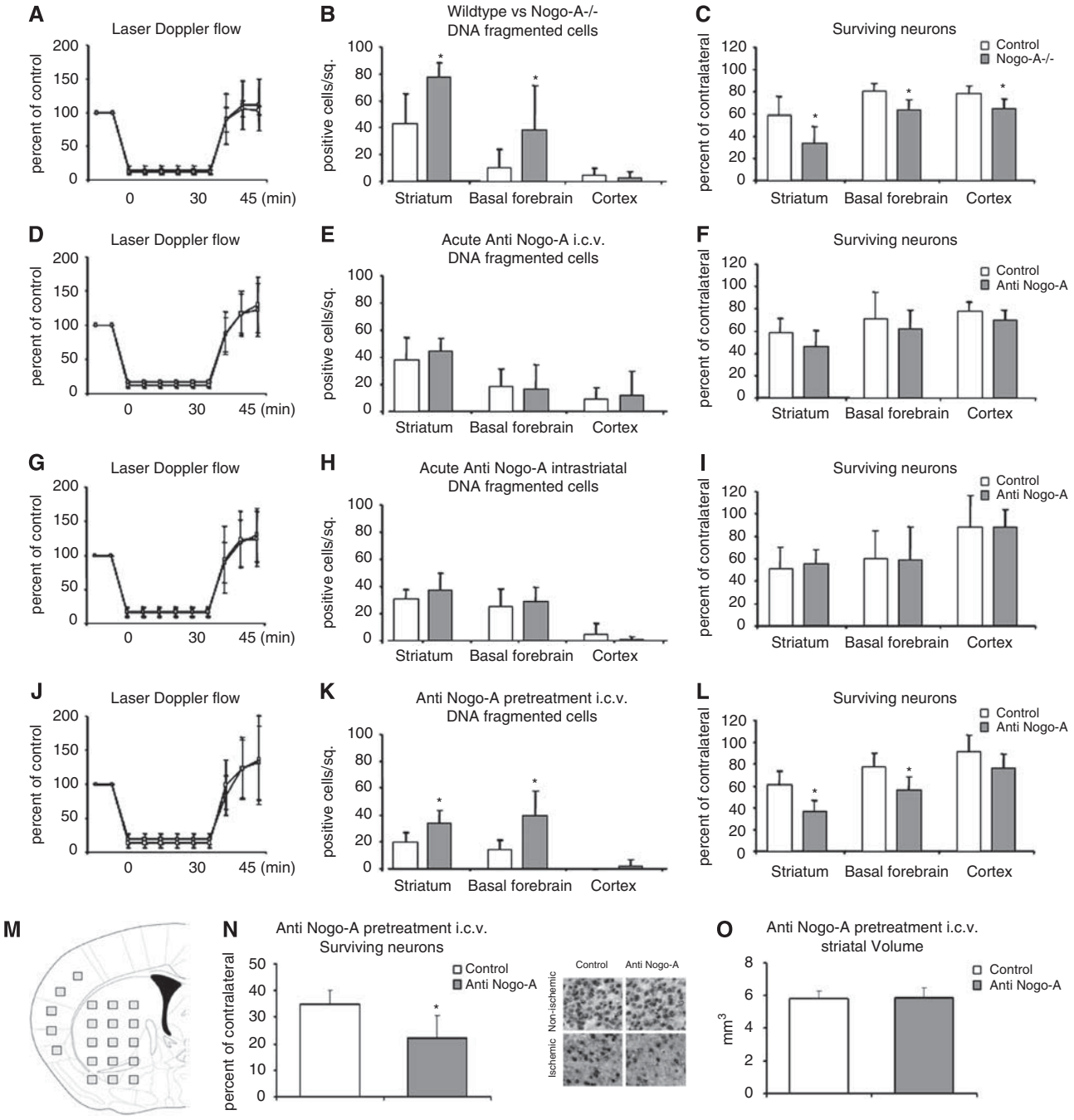

Figure 1 Nogo-A deactivation by genetic knockout and by pre-ischemic, but not post-ischemic delivery of 11C7 antibody compromises neuronal survival after focal cerebral ischemia. The LDF during and after 30 mins MCA occlusion (**A**, **D**, **G**, **J**); density of DNA-fragmented, i.e., injured cells in the ischemic striatum, basal forebrain, and cortex, revealed by TUNEL staining (**B**, **E**, **H**, **K**); percentage of surviving neurons in the same structures, evaluated by NeuN immunohistochemistry (**C**, **F**, **I**, **L**, **N**) and volumetry of the ischemic striatum (**O**). The WT and Nogo-A$^{-/-}$ animals (**A**–**C**), animals treated with control IgG or 11C7 antibody that was delivered into the lateral ventricle (**D**–**F**, **J**–**L**, **N**, **O**) or ischemic striatum (**G**–**I**) starting immediately after reperfusion onset (**D**–**I**) or 24 h before stroke (**J**–**L**, **N**, **O**) are shown, which were assessed by conventional histochemical analysis at 96 or 72 h after reperfusion (**A**–**L**; regions of interest shown in **M**) or by computer-based stereological analysis at 7 days after reperfusion (**N**, **O**). Representative microphotographs of NeuN + neurons are also shown (**N**). Note the absence of differences in LDF recordings between groups (**A**, **D**, **G**). Data are means ± s.d. (**B**–**C**: $n = 8$ animals/group [WT mice]; $n = 5$ animals/group [Nogo-A$^{-/-}$ mice]; **A**, **D**–**L**, **N**, **O**: $n = 8$ animals/group [all groups]). *$P < 0.05$ compared with WT/control IgG-treated groups.

proteins prefixed on colored glutathione sepharose beads (glutathione S-transferase [GST]—p21—activated kinase—Cdc42/Rac interactive binding [GST-PAK-CRIB; PAK02]; GST—rhotekin—Rho-binding domain [GST-RTK-RBD] (RT02); GST—constitutively active Rac1 [GST-Rac1(L61), mutated at L61] (BR02)) were from Cytoskeleton (Frankfurt,

Germany), and anti-Rac1 antibody (05-389) from Upstate (Schwalbach, Germany). Anti-p53 (9282), anti-p75^{NTR} (2693), anti-total (=detecting both unphosphorylated and phosphorylated) Akt (9272), anti-phospho-Akt^{Ser473} (4051), anti-total-phosphatase-and-tensin homolog (PTEN) (9552), anti-phospho-PTEN$^{Ser380/Thr382/383}$ (9554), anti-total-p38/mitogen-activated protein kinase (p38/MAPK) (9212), anti-phospho-p38/MAPK$^{Thr180/Tyr182}$ (9211), anti-total-stress-activated protein kinase/Jun kinase-1/2 (SAPK/JNK1/2) (9252), anti-phospho-SAPK/JNK1/2$^{Thr183/Tyr185}$ (9255), anti-total-extracellular regulated kinase-1/2 (ERK1/2) (9102), anti-phospho-ERK1/2$^{Thr202/Thr204}$ (9101), and anti-β-actin (4967) antibodies were obtained from Cell Signaling (Allschwil, Switzerland).

Protein Extraction and Western Blots: Tissue samples were obtained from the ischemic and contralateral non-ischemic MCA territory, as described earlier (Kilic *et al*, 2006). Tissue samples pooled from animals belonging to the same group were homogenized and lysated in appropriate lysis buffer. In all cases, lysate samples were sonificated over 4 cycles lasting 20 secs each at 4°C at 40% power. Protein concentrations were measured using Bradford assay kit with an iMark Microplate Reader (Bio-Rad, Hercules, CA, USA). For total and phosphorylated protein expression studies, 20 μg of total protein lysates obtained from $MgCl_2$ lysis buffer (50 mmol/L Tris base, 100 mmol/L NaCl, 2 mmol/L $MgCl_2$, 1% NP-40, pH 7.4 and 5% protease inhibitor cocktail) were subjected to SDS–PAGE followed by western blot analysis performed according to the established protocols (Kilic *et al*, 2006), using primary antibodies diluted 1:1000 in 5% skim milk (Sigma) and 0.1 mol/L tris-buffered saline-Triton-X100. Primary antibodies were detected with horseradish peroxidase-conjugated secondary IgG that were diluted 1:5000 in 5% skim milk and tris-buffered saline-Triton-X100 and revealed by enhanced chemiluminescence plus solution (Amersham International, Buckinghamshire, England). Films were digitized and quantified using ImageJ (NIH, USA) image processing software.

Rho GTPase Affinity Binding (Pull Down) Assays: Volumes of equal protein quantities (800 μg) of $MgCl_2$ lysate samples were filled in Eppendorf tubes and complemented to a total volume of 1 mL by adding $MgCl_2$ lysis buffer. For Rac1 affinity binding assays, 20 μL (20 μg) of recombinant GST-PAK-CRIB prefixed to agarose beads were loaded and incubated under slight rotation overnight at 4°C. The next day, samples were centrifuged for 30 secs at 15,000 rpm, and supernatants were dispersed softly and pellets washed three times in ice cold $MgCl_2$ lysis buffer, and a volume of 20 μL of 2× SDS plus 5% 2-mercaptoethanol loading buffer was added to each sample and boiled for 5 mins (Heater Plate, Eppendorf, Germany), then followed by a short centrifugation at 4,000 rpm to precipitate beads. Supernatants from each sample were subjected to SDS–PAGE using 12.5% acrylamide-bis gel. For RhoA and RhoB affinity binding assays, 50 μL (20 μg) of beads-GST-RTK-RBD) were loaded according to the same protocol. For analysis of total Rac1, RhoA and RhoB expression, 20 μg of total protein lysates from each group were subjected to 12.5% SDS–PAGE, followed by western blot analysis.

Interaction of Rock2 with Total and phospho-PTEN, and of Rac1 with JNK1/2 and p38MAPK: Volumes of equal protein quantities (600 μg) of lysate samples obtained from ice cold modified RIPA lysis buffer (consisting of 50 mmol/L Tris-HCl, 150 mmol/L NaCl, 5 mmol/L EDTA, 0.05% NP-40, 1% DOC, 1% Triton X-100, 0.1% SDS [pH 7.4], 0.5% AEBSF [Sigma], 2% AP [Sigma], finally a fresh solution of sodium orthovanadate was added to obtain a final concentration of 1 mmol/L) were added to Eppendorf tubes and diluted with three corresponding volumes of NET buffer (100 mmol/L Tris, 200 mmol/L NaCl, 5 mmol/L EDTA, 5% NP-40, pH 7.4). A volume of 6 μL of total PTEN, phospho-PTEN, or Rac1 antibody was added to each sample, and incubated overnight under slight rotation at 4°C. The next day 20 μL of protein A/G plus-agarose was added to the samples and incubated over 1 h under slight rotation at 4°C. Finally samples were centrifuged for 30 secs at 15,000 rpm at 4°C, supernatants were dispersed and pellets were washed three times in ice cold NET buffer. Samples were processed as described in affinity binding assay protocol, and subjected to SDS–PAGE using 8% or 10% acrylamide-bis gel, followed by western blot analysis for Rock2 as well as total or phospho-SAPK/JNK1/2 and p38/MAPK. For analysis of total Rock2 expression, 20 μg of protein lysates were subjected to 8% SDS–PAGE, followed by western blot analysis.

Co-precipitation Assay with Constitutively Active Rac1: Active Rac1 in its GTP-bound state binds and activates downstream effectors and/or effector complexes. To study interactions of phosphorylated (i.e., activated) SAPK/JNK1/2 and p38/MAPK with Rac1, 50 μL (50 μg) of recombinant GST-Rac1 [L61] prefixed on agarose beads were processed with samples from RIPA buffer lysates (600 μg) as described in the affinity binding assay protocol. Samples were subjected to SDS–PAGE using 10% acrylamide-bis gel, following western blot analysis for phospho-p38/MAPK$^{Thr180/Tyr182}$ and phospho-SAPK/JNK$^{Thr183/Tyr185}$.

Statistics

For statistical analysis, a standard software package (SPSS for Windows 12.1) was used. Values are given as means ± s.d. Differences between groups were compared by two-tailed *t*-tests (comparisons between two groups), one-way ANOVA followed by LSD tests (comparisons between $\geqslant 3$ groups) or repeated measurement ANOVA (comparisons at $\geqslant 2$ time-points), as appropriate. P values < 0.05 were considered significant.

Results

Laser Doppler Flowmetry

To evaluate possible effects of Nogo-A deactivation on brain hemodynamics during and after stroke, we analyzed LDF recordings above the core of the MCA territory. The MCA occlusion resulted in a decrease of LDF levels to ~15% of pre-ischemic values (Figures 1A, 1D, 1G, and 1J). After reperfusion, blood

flow rapidly resumed, reaching levels 15% to 40% above baseline. No differences in LDF were detected between control animals and animals, in which Nogo-A was deactivated, neither by genetic knockout nor by neutralizing antibodies.

Animal Dropouts, Motor and Coordination Deficits, and Spontaneous Locomotor Behavior

In Nogo-A$^{-/-}$ mice, three out of eight animals died before animal sacrifice. As such, one animal was found dead in its cage on day 1 and two animals on day 3 after stroke. In WT mice and in mice receiving antibody infusions, no animal dropouts were noted. In the surviving animals, grip strength tests revealed an exacerbation of motor paresis in the lesion-contralateral right forelimb of Nogo-A$^{-/-}$ compared with WT mice (90.8 ± 12.0 versus $74.3 \pm 15.6\%$ of pre-ischemic baseline in WT and Nogo-A$^{-/-}$ mice, $P < 0.05$). Treatment with the neutralizing Nogo-A antibody 11C7 did not exacerbate motor paresis at 3 days after stroke in the first set of animals studied by conventional histochemistry, both when the antibody delivery was initiated after or before the stroke (grip strength: 84.4 ± 6.0 versus $85.0 \pm 11.5\%$ of baseline for anti-Nogo-A delivery i.c.v. after MCA occlusion; 89.2 ± 13.1 versus $79.5 \pm 12.7\%$ for anti-Nogo-A delivery intrastriatally after MCA occlusion; 84.6 ± 13.4 versus $83.1 \pm 7.3\%$ for anti-Nogo-A delivery i.c.v. 24 h before stroke; all non-significant).

In animals used for a more detailed behavioral analysis, in which the antibody was delivered starting 24 h before MCA occlusion, we observed a more protracted recovery of grip strength and motor coordination in animals receiving the neutralizing Nogo-A antibody. As such, motor force in the paretic right forelimb was significantly reduced in animals receiving 11C7 at 7 days after reperfusion (Figures 2B and 2C). Repeated measurement ANOVA exhibited significant condition $\times$ time interaction effects in grip strength and RotaRod tests, animals receiving the Nogo-A antibody recovering less well from their stroke deficits as compared with control mice (Figures 2B and 2C). In our studies, Nogo-A deactivation did not influence spontaneous locomotor and exploration behavior, as revealed by open field and elevated plus maze tests (Figures 2D and 2E). Body weight was not influenced by 11C7 treatment (Figure 2A).

In all studies, baseline assessments before mini-osmotic pump implantation and MCA occlusion did not differ between groups, both when genetic knockout and antibody deactivation strategies were used.

Absence of Nogo-A in Mice with Constitutive Deletion of Nogo-A-Specific Gene Sequences

To verify the absence of Nogo-A in Nogo-A$^{-/-}$ mice, we next performed western blots, which revealed the presence of 250 kDa Nogo-A in C57Bl/6 WT animals, but not in Nogo-A$^{-/-}$ mice (Figure 3A).

Distribution of Nogo-A Antibody in 11C7-Treated Mice

To characterize the diffusion of the 11C7 antibody in the ischemic brain, we assessed its distribution by immunohistochemistry. This immunohistochemical analysis confirmed the correct localization of antibody infusions. In animals receiving i.c.v. infusions, histochemical stainings revealed the presence of

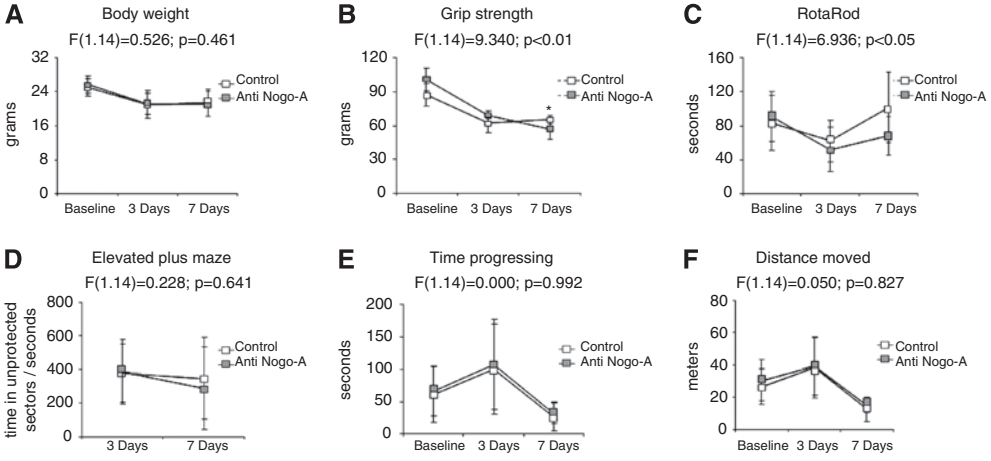

Figure 2 Nogo-A deactivation by neutralizing 11C7 antibody delays neurologic recovery when initiated 24 h before MCA occlusion. Body weight (**A**); grip strength in the paretic right forelimb, as revealed by a spring balance (**B**); motor coordination, as examined on the RotaRod (**C**); and spontaneous locomotor behavior, as evaluated by elevated plus maze (**D**) and open field (**E**, **F**) tests. Note the more protracted recovery of grip strength (**B**) and motor coordination (**C**) in Nogo-A antibody treated as compared with control mice. No differences were seen in spontaneous locomotor and exploration behavior (**D**–**F**). Note that the animals used for this more detailed behavioral analysis differed from those for which behavioural results are presented in the text. Data are means $\pm$ s.d. ($n = 8$ animals per group). *$P < 0.05$ compared with control IgG-treated animals. Condition $\times$ time interaction effects are also shown.

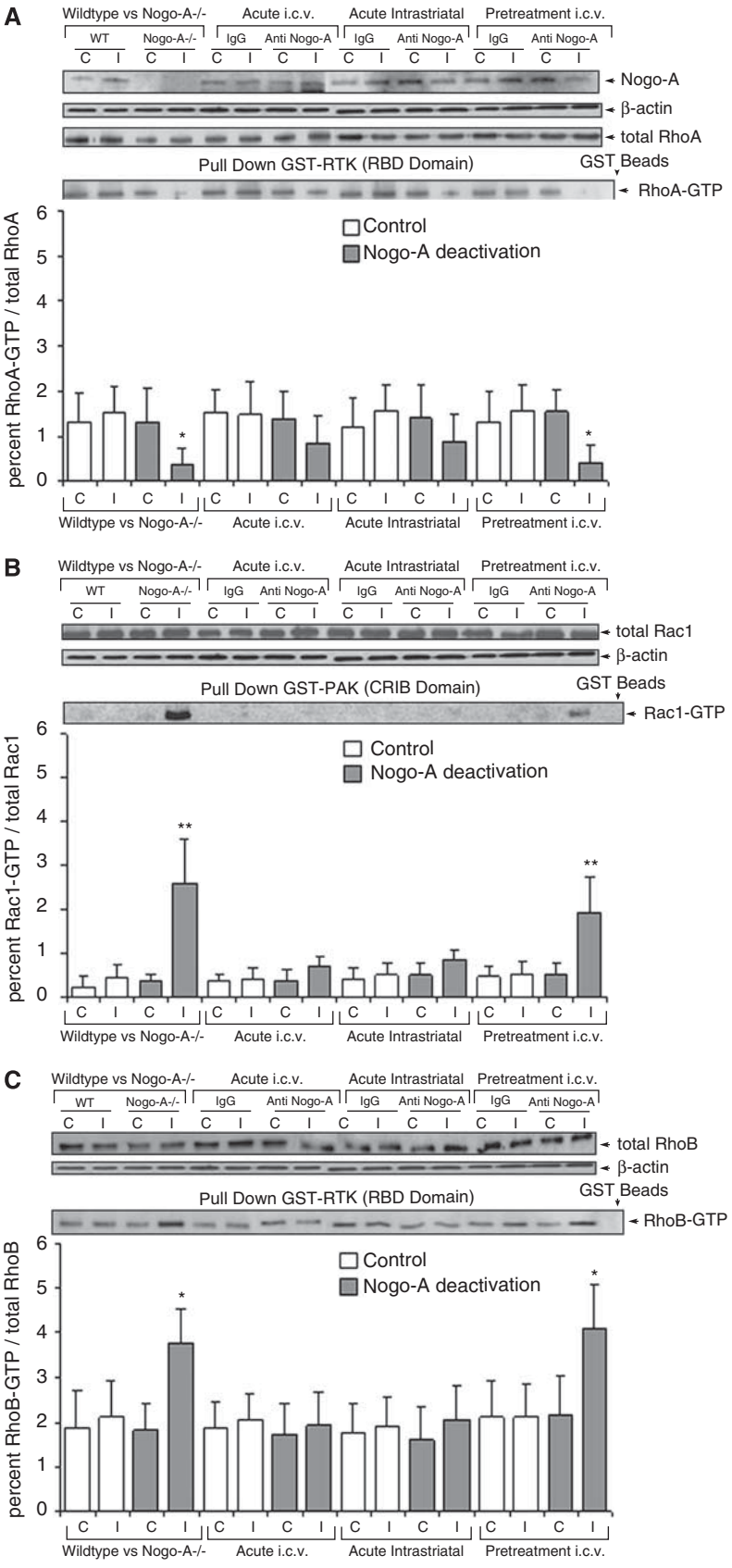
A
Wildtype vs Nogo-A-/-
Acute i.c.v.
Acute Intrastriatal
Pretreatment i.c.v.
WT
Nogo-A-/-
IgG
Anti Nogo-A
C I
Nogo-A
β-actin
total RhoA
Pull Down GST-RTK (RBD Domain)
GST Beads
RhoA-GTP
Control
Nogo-A deactivation
percent RhoA-GTP / total RhoA
B
total Rac1
Pull Down GST-PAK (CRIB Domain)
Rac1-GTP
percent Rac1-GTP / total Rac1
C
total RhoB
Pull Down GST-RTK (RBD Domain)
RhoB-GTP
percent RhoB-GTP / total RhoB

antibody in the dorsomedial parts of the striatum, the cingulate and motor cortex, as well as the septum (Table 1), the more ventral and lateral parts of the striatum and the parietal cortex typically remaining devoid of detectable antibody immunoreactivity. After intrastriatal infusion, almost the entire MCA territory was covered by control IgG and 11C7 (Table 1). No differences in antibody distribution were found between control IgG and anti-Nogo-A antibody 11C7-treated mice (Table 1).

Effects of Nogo-A Deactivation on Neuronal Survival

To evaluate how Nogo-A deactivation influences histopathological injury, we analyzed the density of injured, i.e., TUNEL+ cells and the percentage of surviving neurons in the ischemic striatum, basal forebrain, and cerebral cortex. In Nogo-A$^{-/-}$ mice and in animals treated with 11C7 antibody 24 h before MCA occlusion, deactivation of Nogo-A decreased neuronal survival particularly in the ischemia-vulnerable striatum and basal forebrain. As such, the density of injured cells, evaluated by TUNEL (Figures 1B, 1E, 1H, and 1K), and percentage of surviving neurons, assessed by NeuN immunohistochemistry (Figures 1C, 1F, 1I, and 1L), was similarly affected by Nogo-A deactivation. In contrast to these results, animals receiving 11C7 immediately after ischemia (both after i.c.v. or intrastriatal delivery), Nogo-A inhibition did not influence neuronal viability (Figures 1B, 1C, 1E, 1F, 1H, 1I, 1K, 1L).

To evaluate whether the survival effects of Nogo-A deactivation persisted at later stages of stroke

Table 1 Diffusion distance of control IgG and 11C7 antibody in the ischemic brain, evaluated in the dorsoventral and lateral direction

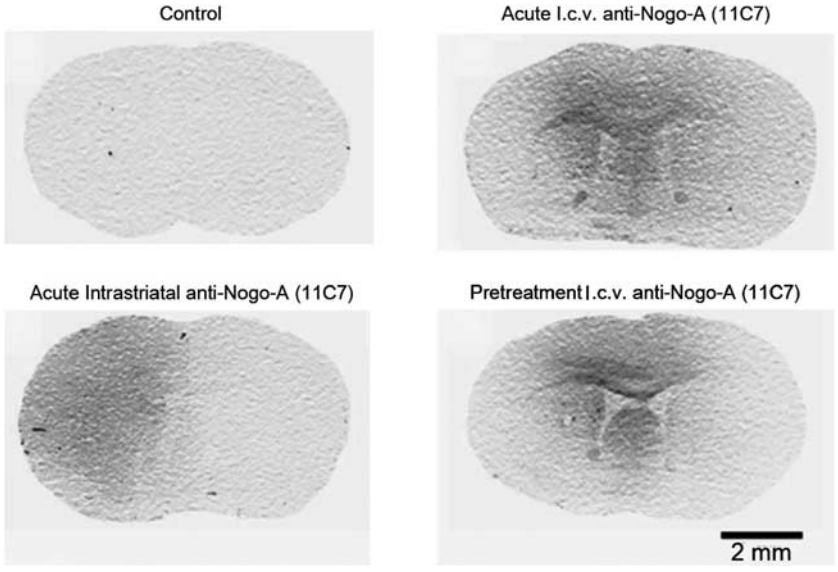

Deactivation strategy	*Dorsoventral (mm)*		*Lateral (mm)*	
	Control	*Nogo-A deactivation*	*Control*	*Nogo-A deactivation*
Genetic Nogo-A$^{-/-}$	n.a.	n.a.	n.a.	n.a.
I.c.v. anti-Nogo-A (11C7) delivery immediately after MCA occlusion	4.9 ± 0.4	5.3 ± 0.5	6.0 ± 0.6	5.2 ± 0.7
Intrastriatal 11C7 delivery immediately after MCA occlusion	5.7 ± 0.8	5.2 ± 0.4	5.6 ± 2.3	4.6 ± 1.1
I.c.v. 11C7 delivery 24 h before MCA occlusion	4.7 ± 0.7	5.1 ± 0.6	5.9 ± 1.1	6.0 ± 1.5

Data are means ± s.d. (WT animals: $n = 8$ animals/group; Nogo-A$^{-/-}$ mice: $n = 5$ animals/group; antibody-treated animals: $n = 8$ animals/group), evaluated at the rostrocaudal level of the striatum. n.a., not applicable.

Figure 3 Nogo-A blockade inhibits the small GTPase RhoA (**A**), at the same time overactivating the small GTPases Rac1 and RhoB in animals exhibiting exacerbated neuronal injury (**B**, **C**). Western blots for Nogo-A, RhoA, Rac1, and RhoB, as well as pull down assays for RhoA, Rac1, and RhoB of ischemic mice exhibiting genetic NogoA-/- as well as animals treated with the Nogo-A antibody 11C7 either immediately after or 24 h before stroke. Note the absence of Nogo-A in NogoA-/- animals (**A**). Blots were normalized with β-actin. RhoA, Rac1, and RhoB activation state was expressed as percent of total protein expression. C, contralateral; I, ischemic. Two blots, of eight samples each, were simultaneously processed and developed, and merged into one figure for further data analysis and presentation. Data are means ± s.d. ($n = 3$ experiments per group). *$P < 0.05$; **$P < 0.01$ compared with corresponding samples of WT/control IgG-treated animals.

recovery, we performed a detailed stereological analysis at 7 days after reperfusion in animals receiving i.c.v. infusions of neutralizing Nogo-A antibody starting 24 h before MCA occlusion. These studies confirmed that Nogo-A deactivation indeed impaired neuronal survival when initiated before the stroke (Figure 1N). Striatal volume was not influenced by 11C7 treatment (Figure 1O).

Both following genetic Nogo-A$^{-/-}$ and antibody-mediated Nogo-A blockade, neuronal densities in the ischemia-contralateral striatum did not differ between groups (not shown). Thus, there were no indications for toxic side-effects of Nogo-A deactivation in non-ischemic brain tissue.

Effect of Nogo-A Deactivation on Small GTPases RhoA, Rac1, and RhoB

To understand how Nogo-A deactivation influences cell survival, we examined the expression and activation of small GTPases RhoA and Rac1, which mediate Nogo-A's outgrowth inhibitory effect via activation (RhoA) and deactivation (Rac1), respectively (Niederöst *et al*, 2002; Kubo *et al*, 2007). Interestingly, RhoA activation was particularly strongly decreased in brain ischemic tissue of Nogo-A$^{-/-}$ mice and of mice receiving Nogo-A antibodies before MCA occlusion (Figure 3A), as shown in pull down studies using GST-RTK-RBD. On the other hand, Rac1 was excessively activated in the latter animals that exhibited impaired neuronal survival due to Nogo-A deactivation (Figure 3B), as shown in GST-PAK-CRIB pull downs. RhoB, which has been described as an early predictor of neuronal death (Trapp *et al*, 2001), was also overactivated, similar to Rac1, in ischemic tissue of animals with reduced cell survival. The overall expression of RhoA, Rac1, and RhoB remained unchanged after Nogo-A deactivation (Figure 3C). Our results show that Nogo-A deactivation differentially regulates the activation of the Rho GTPases RhoA, Rac1, and RhoB.

p38/MAPK and SAPK/JNK1/2 Activation After Nogo-A Blockade is Controlled by Rac1

The stress kinases p38/MAPK and SAPK/JNK1/2 have been described as downstream targets of Rho GTPase effectors (Tibbles *et al*, 1996; Muñoz-Alonso *et al*, 2008). Indeed, western blot analysis showed significantly increased levels of phosphorylated (i.e., activated), but not overall p38/MAPK and SAPK/JNK1/2 in the ischemic tissue of animals exhibiting reduced neuronal survival due to Nogo-A deactivation (Figures 4A–4C). Specifically in ischemic tissue, immunoprecipitation and co-precipitation studies revealed that phosphorylated p38/MAPK and SAPK/JNK1/2 interacted with active Rac1, forming complexes under conditions in which neuronal survival was compromised (Figure 4D). Our data suggest that p38/MAPK and SAPK/JNK1/2 are direct downstream targets of active Rac1.

RhoA/Rock2 Deactivation Results in PTEN Activation, Furthermore Downregulating Akt and ERK1/2

The phosphatase PTEN controls the phosphorylation and activation of the survival kinases Akt and ERK1/2 pathways via downstream effectors (Ning *et al*, 2004; Gu *et al*, 1998). Using western blots analysis, we found that the phosphorylation but not total expression of PTEN was decreased (its activity being increased) (Figure 5A), similarly as the phosphorylation but not overall expression of Akt and ERK1/2 was decreased (their activity being decreased) by Nogo-A deactivation (Figures 5B–5D). Immunoprecipitation studies showed that PTEN was present in a Rock2-bound state in control animals and that Rock2-bound PTEN was almost completely dephosphorylated (i.e., activated) in response to Nogo-A deactivation (Figure 5E). Our data indicate that Rock2 controls the PTEN activation.

p53 Expression is Increased in Nogo-A Deactivated Groups

Akt enhances cell survival partly by sequestering and ubiquitinylating the death protein p53 (Gottlieb *et al*, 2002). Western blot analysis revealed increased p53 expression in animals exhibiting decreased neuronal survival due to Nogo-A deactivation (Figure 5F). Notably in the antibody-treated groups, the p53 pathway was activated only when the 11C7 antibody was delivered before, but not after the stroke, thus confirming that Nogo-A inhibition was harmful only when initiated before ischemia.

Discussion

Animal studies have recently reinvigorated hopes that by use of neutralizing antibodies targeting the growth-inhibitory Nogo-A protein functional neurologic recovery in spinal cord injury (Schnell and Schwab, 1990; Bregman *et al*, 1995; Merkler *et al*, 2001; Liebscher *et al*, 2005; Freund *et al*, 2006) and ischemic stroke (Papadopoulos *et al*, 2002; Wiessner *et al*, 2003; Markus *et al*, 2005; Seymour *et al*, 2005) may clinically be improved. Compared with acute neuroprotection therapies, which without exception, failed in proof-of-concept trials in human patients (O'Collins *et al*, 2006; Savitz and Fisher, 2007), the reinforcement of fiber regeneration and structural plasticity, reflects a paradigm change, as the acute phase of injury is no more the focus of interest. This opens therapeutic perspectives for large patient groups, as treatment is no more restricted to narrow time windows. In fact, treatment may successfully be initiated even days, perhaps weeks after a stroke, based on animal data (Markus *et al*, 2005; Seymour *et al*, 2005). In view of the strong promises related to

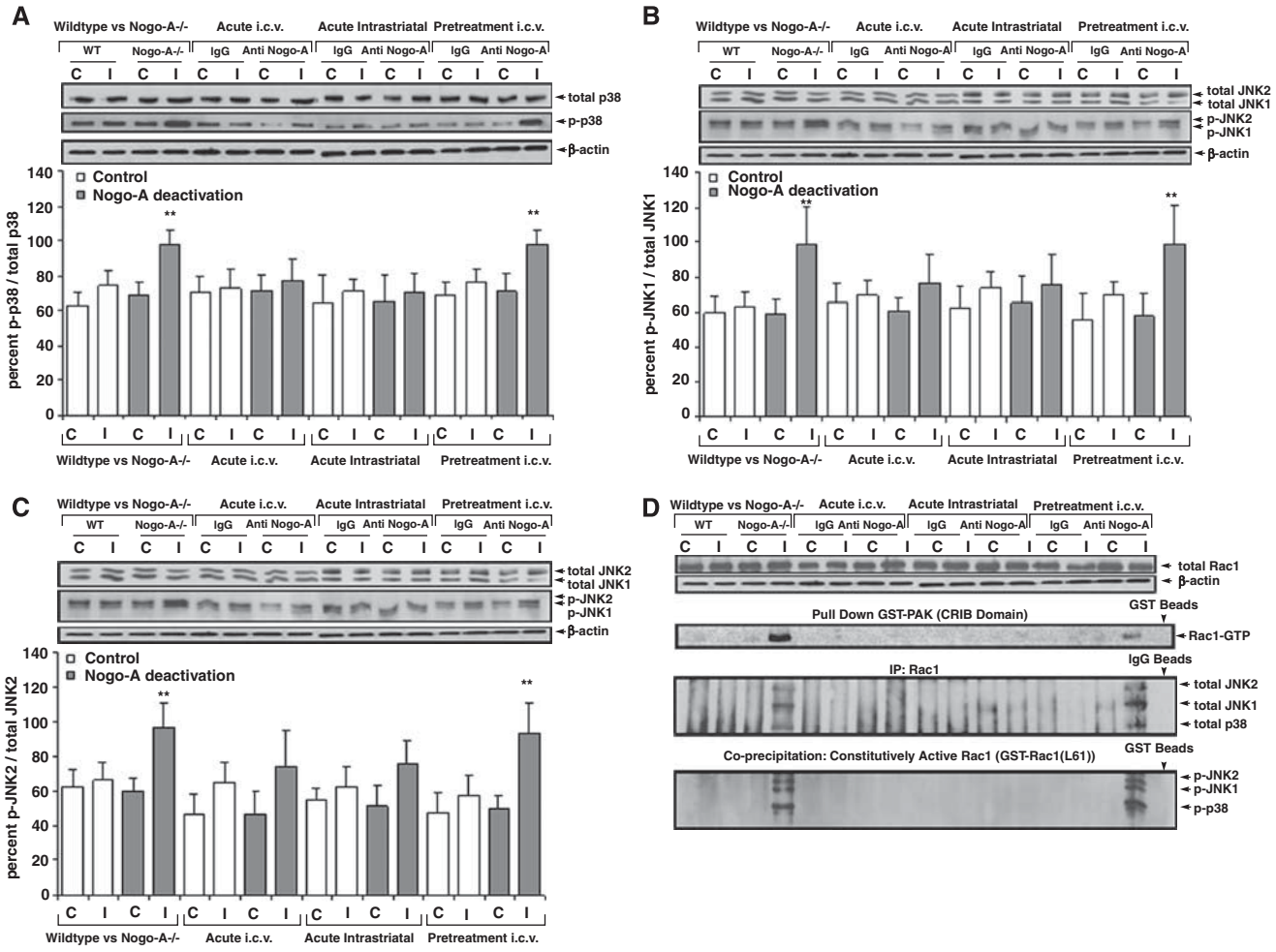

Figure 4 Nogo-A inhibition activates the p38/MAPK and SAPK/JNK1/2 pathways via direct interaction with active Rac1. Western blots using antibodies detecting either phosphorylated (p-p38, p-JNK1/2) or total (= overall; i.e., phosphorylated and non-phosphorylated) p38/MAPK (**A**) and SAPK/JNK1/2 (**B**, **C**), as well as immunoprecipitation and co-precipitation studies examining protein interactions of total p38/MAPK and total SAPK/JNK1/2 with Rac1, and of phosphorylated p38/MAPK and phosphorylated SAPK/JNK1/2 with constitutively active GST-Rac1 (L61) (**D**). Blots were normalized with β-actin and expressed as ratio between phosphorylated and total stress kinases. C, contralateral; I, ischemic. Two blots, of eight samples each, were simultaneously processed and developed, and merged for further data analysis and presentation. Data are means ± s.d. ($n = 3$ experiments per group). $^{**}P < 0.01$ compared with corresponding samples of WT/control IgG-treated animals.

Nogo-A neutralizing therapies, clinical proof-of-concept trials are presently on their way for spinal cord injury.

In addition to its growth inhibitory actions, we herein found a novel neuronal survival-promoting effect of Nogo-A, which has not been reported until now. Neuronal survival was compromised in the striatum and basal forebrain, but less so in the cortex of mice constitutively ablated for the Nogo-A gene or mice pretreated with a function blocking anti-Nogo-A antibody starting 24 h before the stroke. Conversely, no effects on neuronal survival were seen in animals treated with anti-Nogo-A antibodies after the stroke. That survival effects of Nogo-A have not been described may have to do with the fact that neutralizing antibodies directed against this growth inhibitor have so far been tested only in models of permanent focal cerebral ischemia, e.g., transcranial MCA electrocoagulation (Wiessner *et al*, 2003; Lee *et al*, 2004; Markus *et al*, 2005), MCA ligation (Seymour *et al*, 2005) or photothrombotic cortical injury (Wiessner *et al*, 2003; Lee *et al*, 2004), antibody application starting acutely or with delays of days after the stroke. In skilled hands, transcranial MCA occlusion and photothrombotic lesions induce very uniform brain infarcts, in which the entire tissue territory supplied by the occluded arteries is lost. As a matter of fact, brain damage can hardly be exacerbated under such conditions. The question arises whether Nogo-A deactivation may also induce cell injury under conditions other than ischemia, as well as in the intact brain. Future studies will have to address this issue.

Using a broad set of protein expression and interaction studies, we identified specific signaling pathways underlying Nogo-A's survival-promoting

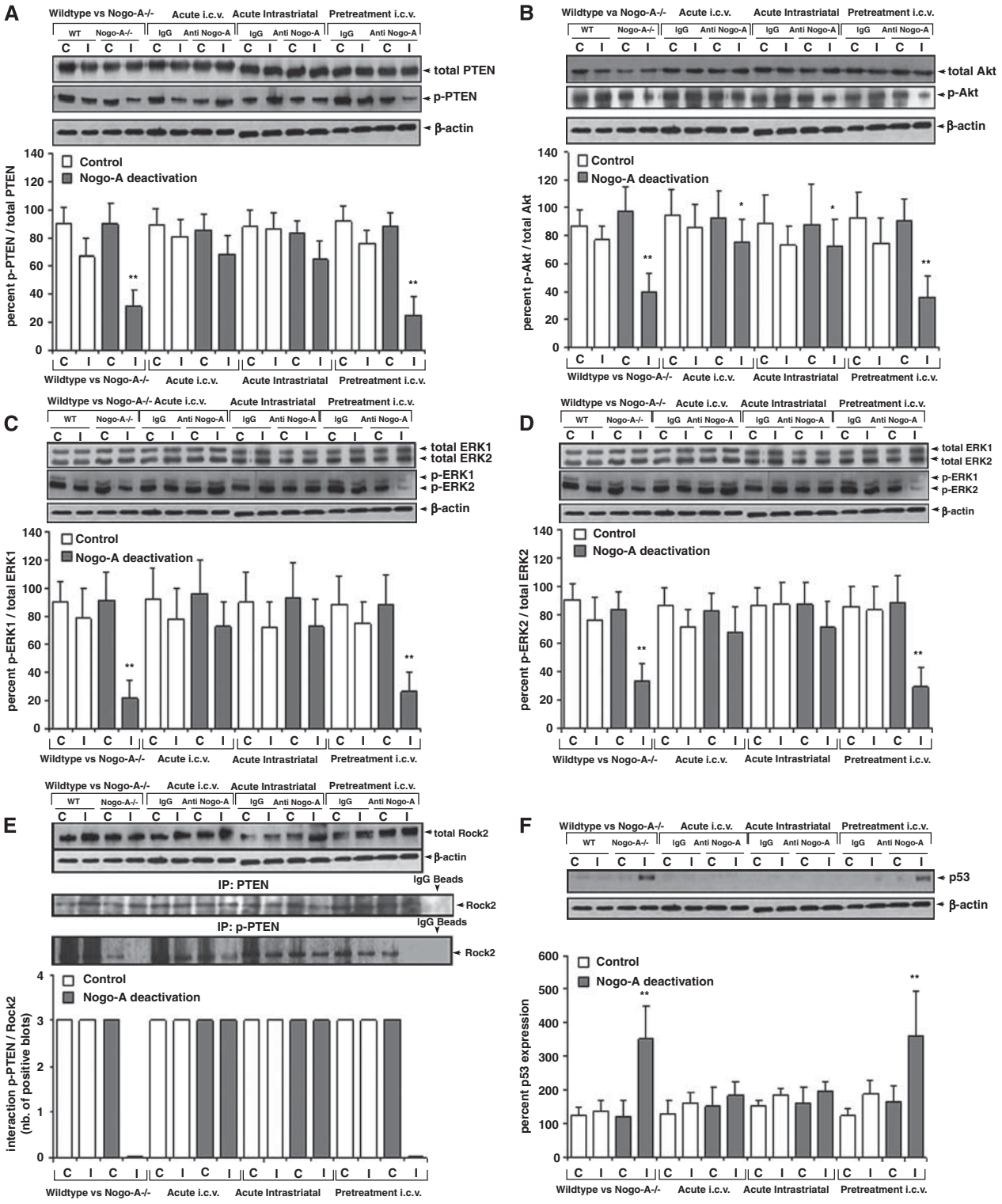

Figure 5 Nogo-A blockade deactivates Rock2, decreasing PTEN phosphorylation and activating it, thus dephosphorylating and deactivating Akt and ERK1/2 pathways and inducing the p53 death pathway. Western blots using antibodies detecting either phosphorylated (p-PTEN, p-Akt, p-ERK1/2) or total (i.e., phosphorylated and non-phosphorylated) PTEN, Akt, and ERK1/2 (**A**–**D**), immunoprecipitation studies examining protein interactions of total and phosphorylated PTEN with Rock2 (**E**) and western blots for the death protein p53 (**F**). Blots were normalized with β-actin and expressed as ratio between phosphorylated and total signal proteins. C, contralateral; I, ischemic. Two blots, of eight samples each, were simultaneously processed and developed, and merged for further data analysis and presentation. Data are means ± s.d. ($n = 3$ experiments per group). $^{*}P < 0.05$; $^{**}P < 0.01$ compared with corresponding samples of WT/control IgG-treated animals.

effects. As such, we noticed an overactivation of Rac1 in animals exhibiting exacerbated neuronal injury due to NogoA blockade, which in turn stimulated the p38/MAPK and SAPK/JNK1/2 stress pathways via direct interaction (Figure 6). Indeed, our observation that active Rac1 formed a complex with both p38/MAPK and SAPK/JNK1/2 indicates that Rac1 itself controls the activation of the stress response. p38/MAPK and SAPK/JNK1/2 have previously been shown to act as downstream targets of Rho GTPase effectors *in vitro* (Tibbles *et al*, 1996; Muñoz-Alonso *et al*, 2008). That both stress kinases specifically bind to Rac1 was unknown.

On the other hand, RhoA deactivation stimulated the phosphatase PTEN via its downstream effector Rock2, which deactivated the survival factors Akt and ERK1/2, finally resulting in the activation of p53-dependent death pathways (Figure 6). Rock has been shown to regulate cell survival in the central nervous system. Rock exists in two isoforms, Rock1 and Rock2, which share 92% homology in their kinase domain (Wei *et al*, 2001). Among these isoforms, Rock2 is particularly strongly expressed in the brain (Wei *et al*, 2001). For Rock1, it has already been described *in vitro* that the kinase phosphorylates PTEN in its C2 domain, whereas almost all other kinases phosphorylate PTEN at its C-terminus thus deactivating it (Li *et al*, 2005; Chang *et al*, 2006; Gericke *et al*, 2006). In case of Rock2, direct interactions with PTEN have never been shown *in vivo*. Our observation of PTEN being phosphorylated and deactivated at its C-terminus in the presence of Rock2 argues in favor of differential roles of both Rock isoforms, or of Rock2 interaction with intermediate proteins that control PTEN phosphorylation. These two hypotheses should further be analyzed in the future.

That PTEN deactivates the phosphatidyl-inositol-3-kinase (PI3K)/Akt and mitogen-activated protein kinase kinase (MEK)/ERK1/2 pathways (Ning *et al*, 2004; Gu *et al*, 1998) is well established. The PI3K/Akt, on the other hand, is known to stimulate p53 degradation via phosphorylation of Mdm2 *in vitro* (Gottlieb *et al*, 2002). By showing that PTEN, Akt, and ERK1/2 were synergistically desphosphorylated, while p53 was overexpressed, in response to Nogo-A deactivation, we now for the first time provide evidence that the PTEN/Akt/p53 and PTEN/MEK/ERK1/2 pathways are regulated by Nogo-A and are involved in the regulation of neuronal survival *in vivo*. Thus, our data offer new insights how survival signals are mediated in the ischemic brain.

In our studies, Nogo-A deactivation both by genetic deletion or neutralizing antibodies exacerbated functional neurologic deficits. As such, Nogo-A$^{-/-}$ animals revealed more severe deficits than WT mice, and behavioral recovery was more protracted in animals treated with Nogo-A antibody as compared with control antibody-treated animals. That neurologic performance is more strongly compromised in ischemic animals exhibiting Nogo-A deactivation exemplifies that the survival effects we found are functionally relevant. The behavioral phenotype of Nogo-A$^{-/-}$ animals has recently been characterized in detail by Willi *et al* (2009), who did not find major neurologic deficits in healthy Nogo-A$^{-/-}$ mice. In comparison to WT animals, motor coordination was even enhanced, which was

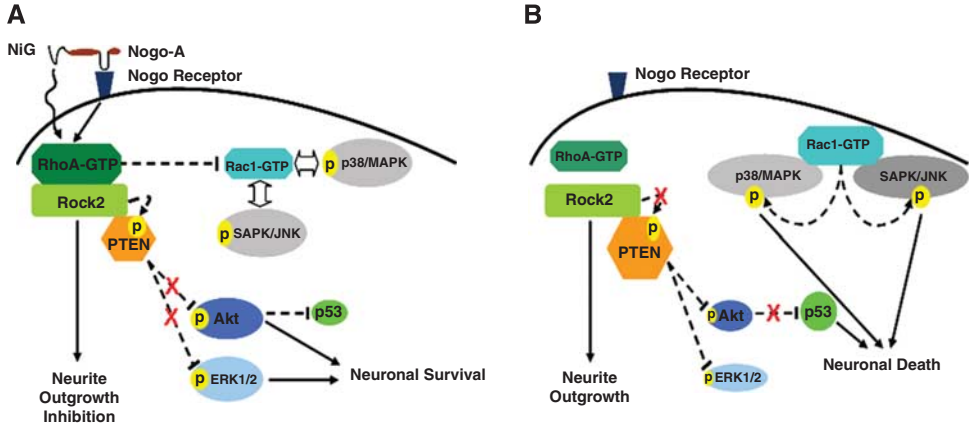

Figure 6 Scheme outlining the novel role of Nogo-A in controlling neuronal survival in the ischemic brain. When Nogo-A signaling pathway is active, through the putative receptor and/or directly through its N-terminal inhibitory region (NiG) (as shown in **A**), the small GTPase RhoA is active, whereas the Rho GTPases members Rac1 and RhoB are inactive. As a consequence of Rac1 inactivation, the p38/MAPK and SAPK/JNK1/2 pathways are inhibited, and PTEN activity is controlled and maintained low by increasing its phosphorylation via Rock2, and the PI3K/Akt and ERK1/2 pathways are active, thus enhancing p53 degradation and promoting neuronal survival. Nogo-A signaling inhibition, on the other hand (as shown in **B**), deactivates RhoA, at the same time overactivates Rac1 and RhoB, the former of which mediates the activation of the p38/MAPK and SAPK/JNK1/2 stress response via direct interaction. Deactivation of RhoA, as a consequence of Nogo-A inhibition, inactivates its direct downstream effector Rock2, therefore the latter looses PTEN phosphorylation control, whereby the PTEN phosphatase is activated, which in turn deactivates PI3K/Akt and ERK1/2 pathways and induces death signaling by stabilizing p53. Black complete lines were used for direct signaling pathways, and black dashed lines were used for indirect signaling pathways.

interpreted as correlate of the enhanced brain plasticity of these animals. In spinal cord trauma (Freund *et al*, 2006) and permanent focal cerebral ischemia (Wiessner *et al*, 2003), Nogo-A deactivation with neutralizing antibodies improves behavioral neurologic deficits. Impaired motor and cognitive recovery has recently been shown after traumatic brain injury in mice exhibiting combined Nogo-A/B$^{-/-}$ (Marklund *et al*, 2009). Whether the exacerbated recovery in that mouse line is also attributed to exacerbated neuronal injury, still remains to be shown.

The here-reported survival-promoting effect of Nogo-A is corroborated by observations in Drosophila, where loss-of-function mutations of the only *nogo/reticulon* gene, *reticulon-like 1*, reduced the life expectancy of flies (Wakefield and Tear, 2006). Our findings have no direct relevancy with respect to presently ongoing clinical trials in human patients using neutralizing Nogo-A antibodies, as neuronal survival was altered only when antibodies were delivered before the stroke. Importantly, when delivered after ischemia, Nogo-A antibodies did not influence neuronal survival, both when applied into the lateral ventricle or directly into the mouse striatum. In human patients, the duration of ischemia is less well defined compared with experimental conditions, reperfusion latencies ranging from minutes to hours or even days after stroke in individual patients. On the basis of these results, care should be taken not to deliver Nogo-A antibodies in the very early stroke phase, under conditions of persistent/recurrent ischemia. Post-acute delivery strategies may help to rule out undesirable effects of Nogo-A deactivation strategies.

To ensure the successful translation of Nogo-A antibodies from the bench to the clinic, growth-promoting therapies should not repeat mistakes of earlier neuroprotection trials, i.e., to neglect bystander effects of treatments. As such, plasticity-promoting therapies should be aware of possible neuronal survival effects in the acute stroke phase, which should be carefully analyzed. With such precaution, chances appear favorable that plasticity-promoting strategies might lead stroke therapies to new breakthroughs.

Acknowledgements

We thank B Karow and E Cam for technical assistance. This work was supported by the NCCR 'Neural plasticity and repair,' Swiss National Science Foundation (3200B0-112056), Deutsche Forschungsgemeinschaft (HE3173/2-1), Roche Foundation for Anemia Research (RoFAR), Heinz Nixdorf Foundation, Jackstädt Foundation (all to DMH), and an EMBO installation grant (to EK).

Disclosure/conflict of interest

The authors declare no conflict of interest.

References

Acevedo L, Yu J, Erdjument-Bromage H, Miao RQ, Kim JE, Fulton D, Tempst P, Strittmatter SM, Sessa WC (2004) A new role for Nogo as a regulator of vascular remodeling. *Nat Med* 10:382–8

Bacigaluppi M, Pluchino S, Jametti LP, Kilic E, Kilic U, Salani G, Brambilla E, West MJ, Comi G, Martino G, Hermann DM (2009) Delayed post-ischaemic neuroprotection following systemic neural stem cell transplantation involves multiple mechanisms. *Brain* 32:2239–51

Bergh F, van den Spronk M, Ferreira L, Bloemarts E, Groenink L, Olivier B, Oosting R (2007) Relationship of delay aversion and response inhibition to extinction learning, aggression, and sexual behaviour. *Behav Brain Res* 175:75–81

Bregman BS, Kunkel-Bagden E, Schnell L, Dai HN, Gao D, Schwab ME (1995) Recovery from spinal cord injury mediated by antibodies to neurite growth inhibitors. *Nature* 378:498–501

Buchli AD, Schwab ME (2005) Inhibition of Nogo: a key strategy to increase regeneration, plasticity and functional recovery of the lesioned central nervous system. *Ann Med* 37:556–67

Chang J, Xie M, Shah VR, Schneider MD, Entman ML, Wei L, Schwartz RJ (2006) Activation of Rho-associated coiled-coil protein kinase 1 (ROCK-1) by caspase-3 cleavage plays an essential role in cardiac myocyte apoptosis. *Proc Natl Acad Sci USA* 103:14495–500

Chen MS, Huber AB, van der Haar ME, Frank M, Schnell L, Spillmann AA, Christ F, Schwab ME (2000) Nogo-A is a myelin-associated neurite outgrowth inhibitor and an antigen for monoclonal antibody IN-1. *Nature* 403:434–9

Dimou L, Schnell L, Montani L, Duncan C, Simonen M, Schneider R, Liebscher T, Gullo M, Schwab ME (2006) Nogo-A-deficient mice reveal strain-dependent differences in axonal regeneration. *J Neurosci* 26: 5591–603

Freund P, Schmidlin E, Wannier T, Bloch J, Mir A, Schwab ME, Rouiller EM (2006) Nogo-A-specific antibody treatment enhances sprouting and functional recovery after cervical lesion in adult primates. *Nat Med* 12:790–2

Gottlieb TM, Leal JF, Seger R, Taya Y, Oren M (2002) Cross-talk between Akt, p53 and Mdm2: possible implications for the regulation of apoptosis. *Oncogene* 21:1299–303

Gericke A, Munson M, Ross AH (2006) Regulation of the PTEN phosphatase. *Gene* 374:1–9

GrandPre T, Nakamura F, Vartanian T, Strittmatter SM (2000) Identification of the Nogo inhibitor of axon regeneration as a Reticulon protein. *Nature* 403:439–44

Gu J, Tamura M, Yamada KM (1998) Tumor suppressor PTEN inhibits integrin- and growth factor-mediated mitogen-activated protein (MAP) kinase signaling pathways. *J Cell Biol* 143:1375–83

Harel NY, Strittmatter SM (2006) Can regenerating axons recapitulate developmental guidance during recovery from spinal cord injury? *Nat Rev Neurosci* 7:603–16

Hermann DM, Kilic E, Hata R, Hossmann KA, Mies G (2001) Relationship between metabolic dysfunctions, gene responses and delayed cell death after mild focal cerebral ischemia in mice. *Neuroscience* 104:947–55

Kilic E, Kilic Ü, Soliz J, Bassetti CL, Gassmann M, Hermann DM (2005) Brain-derived erythropoietin protects from focal cerebral ischemia by dual activation of ERK-1/-2 and Akt pathways. *FASEB J* 19:2026–8

Kilic E, Kilic Ü, Wang Y, Bassetti CL, Marti HH, Hermann DM (2006) The phosphatidylinositol-3 kinase/Akt pathway mediates VEGF's neuroprotective activity and induces blood brain barrier permeability after focal cerebral ischemia. *FASEB J* 20:1185–7

Kilic E, Kilic Ü, Bacigaluppi M, Guo Z, Abdallah NB, Wolfer DP, Reiter RJ, Hermann DM, Bassetti CL (2008) Delayed melatonin administration promotes neuronal survival, neurogenesis and motor recovery, and attenuates hyperactivity and anxiety after mild focal cerebral ischemia in mice. *J Pineal Res* 45:142–8

Kubo T, Hata K, Yamaguchi A, Yamashita T (2007) Rho-ROCK inhibitors as emerging strategies to promote nerve regeneration. *Curr Pharm Des* 13: 2493–9

Lee JK, Kim JE, Sivula M, Strittmatter SM (2004) Nogo receptor antagonism promotes stroke recovery by enhancing axonal plasticity. *J Neurosci* 24:6209–17

Li Z, Dong X, Wang Z, Liu W, Deng N, Ding Y, Tang L, Hla T, Zeng R, Li L, Wu D (2005) Regulation of PTEN by Rho small GTPases. *Nat Cell Biol* 7:399–404

Liebscher T, Schnell L, Schnell D, Scholl J, Schneider R, Gullo M, Fouad K, Mir A, Rausch M, Kindler D, Hamers FP, Schwab ME (2005) Nogo-A antibody improves regeneration and locomotion of spinal cord-injured rats. *Ann Neurol* 58:706–19

Marklund N, Morales D, Clausen F, Hånell A, Kiwanuka O, Pitkänen A, Gimbel DA, Philipson O, Lannfelt L, Hillered L, Strittmatter SM, McIntosh TK (2009) Functional outcome is impaired following traumatic brain injury in aging Nogo-A/B-deficient mice. *Neuroscience* 163:540–51

Markus TM, Tsai SY, Bollnow MR, Farrer RG, O'Brien TE, Kindler-Baumann DR, Rausch M, Rudin M, Wiessner C, Mir AK, Schwab ME, Kartje GL (2005) Recovery and brain reorganization after stroke in adult and aged rats. *Ann Neurol* 58:950–3

McGee AW, Strittmatter SM (2003) The Nogo-66 receptor: focusing myelin inhibition of axon regeneration. *Trends Neurosci* 26:193–8

Merkler D, Metz GA, Raineteau O, Dietz V, Schwab ME, Fouad K (2001) Locomotor recovery in spinal cord-injured rats treated with an antibody neutralizing the myelin-associated neurite growth inhibitor Nogo-A. *J Neurosci* 21:3665–73

Muñoz-Alonso MJ, González-Santiago L, Zarich N, Martínez T, Alvarez E, Rojas JM, Muñoz A (2008) Plitidepsin has a dual effect inhibiting cell cycle and inducing apoptosis via Rac1/c-Jun NH2-terminal kinase activation in human melanoma cells. *J Pharmacol Exp Ther* 324:1093–101

Niederöst B, Oertle T, Fritsche J, McKinney RA, Bandtlow CE (2002) Nogo-A and myelin-associated glycoprotein mediate neurite growth inhibition by antagonistic regulation of RhoA and Rac1. *J Neurosci* 22:10368–76

Ning K, Pei L, Liao M, Liu B, Zhang Y, Jiang W, Mielke JG, Li L, Chen Y, El-Hayek YH, Fehlings MG, Zhang X, Liu F, Eubanks J, Wan Q (2004) Dual neuroprotective signaling mediated by downregulating two distinct phosphatase activities of PTEN. *J Neurosci* 24:4052–60

O'Collins VE, Macleod MR, Donnan GA, Horky LL, van der Worp BH, Howells DW (2006) 1,026 experimental treatments in acute stroke. *Ann Neurol* 59:467–77

Oertle T, van der Haar ME, Bandtlow CE, Robeva A, Burfeind P, Buss A, Huber AB, Simonen M, Schnell L, Brösamle C, Kaupmann K, Vallon R, Schwab ME (2003) Nogo-A inhibits neurite outgrowth and cell spreading with three discrete regions. *J Neurosci* 23:5393–406

Papadopoulos CM, Tsai SY, Alsbiei T, O'Brien TE, Schwab ME, Kartje GL (2002) Functional recovery and neuroanatomical plasticity following middle cerebral artery occlusion and IN-1 antibody treatment in the adult rat. *Ann Neurol* 51:433–41

Savitz SI, Fisher M (2007) Future of neuroprotection in the aftermath of the SAINT trials. *Ann Neurol* 61: 396–402

Schnell L, Schwab ME (1990) Axonal regeneration in the rat spinal cord produced by an antibody against myelin-associated neurite growth inhibitors. *Nature* 343:269–72

Schwab ME (2004) Nogo and axon regeneration. *Curr Opin Neurobiol* 14:118–24

Seymour AB, Andrews EM, Tsai SY, Markus TM, Bollnow MR, Brenneman MM, O'Brien TE, Castro AJ, Schwab ME, Kartje GL (2005) Delayed treatment with monoclonal antibody IN-1 1 week after stroke results in recovery of function and corticorubral plasticity in adult rats. *J Cereb Blood Flow Metab* 25:1366–75

Simonen M, Pedersen V, Weinmann O, Schnell L, Buss A, Ledermann B, Christ F, Sansig G, van der Putten H, Schwab ME (2003) Systemic deletion of the myelin-associated outgrowth inhibitor Nogo-A improves regenerative and plastic responses after spinal cord injury. *Neuron* 38:201–11

Spudich A, Kilic E, Xing H, Kilic Ü, Rentsch KM, Wunderli-Allenspach H, Bassetti CL, Hermann DM (2006) Inhibition of multidrug resistance transporter-1 facilitates neuroprotective therapies after focal cerebral ischemia. *Nat Neurosci* 9:487–8

Sugiura S, Kitagawa K, Tanaka S, Todo K, Omura-Matsuoka E, Sasaki T, Mabuchi T, Matsushita K, Yagita Y, Hori M (2005) Adenovirus-mediated gene transfer of heparin-binding epidermal growth factor-like growth factor enhances neurogenesis and angiogenesis after focal cerebral ischemia in rats. *Stroke* 36:859–64

Tibbles LA, Ing YL, Kiefer F, Chan J, Iscove N, Woodgett JR, Lassam NJ (1996) MLK-3 activates the SAPK/JNK and p38/RK pathways via SEK1 and MKK3/6. *EMBO J* 15:7026–35

Trapp T, Oláh L, Hölker I, Besselmann M, Tiesler C, Maeda K, Hossmann KA (2001) GTPase RhoB: an early predictor of neuronal death after transient focal ischemia in mice. *Mol Cell Neurosci* 17:883–94

Tremml P, Lipp HP, Müller U, Ricceri L, Wolfer DP (1998) Neurobehavioral development, adult openfield exploration and swimming navigation learning in mice with a modified beta-amyloid precursor protein gene. *Behav Brain Res* 95:65–76

Wakefield S, Tear G (2006) The Drosophila reticulon, Rtnl-1, has multiple differentially expressed isoforms that are associated with a sub-compartment of the endoplasmic reticulum. *Cell Mol Life Sci* 63:2027–38

Wang Y, Kilic E, Kilic Ü, Weber B, Bassetti CL, Marti HH, Hermann DM (2005) VEGF overexpression induces post-ischaemic neuroprotection, but facilitates haemodynamic steal phenomena. *Brain* 128:52–63

Wei L, Roberts W, Wang L, Yamada M, Zhang S, Zhao Z, Rivkees SA, Schwartz RJ, Imanaka-Yoshida K (2001) Rho kinases play an obligatory role in vertebrate embryonic organogenesis. *Development* 128: 2953–62

Wiessner C, Bareyre FM, Allegrini PR, Mir AK, Frentzel S, Zurini M, Schnell L, Oertle T, Schwab ME (2003) Anti-Nogo-A antibody infusion 24 h after

experimental stroke improved behavioral outcome and corticospinal plasticity in normotensive and spontaneously hypertensive rats. *J Cereb Blood Flow Metab* 23:154–65

Willi R, Aloy EM, Yee BK, Feldon J, Schwab ME (2009) Behavioral characterization of mice lacking the neurite outgrowth inhibitor Nogo-A. *Genes Brain Behav* 8:181–92

Yiu G, He Z (2006) Glial inhibition of CNS axon regeneration. *Nat Rev Neurosci* 7:617–27

Young EJ, Lipina T, Tam E, Mandel A, Clapcote SJ, Bechard AR, Chambers J, Mount HTJ, Fletcher PJ, Roder JC, Osborne LR (2008) Reduced fear and aggression and altered serotonin metabolism in Gtf2ird1-targeted mice. *Genes Brain Behav* 7:224–34